

## An ESR and ENDOR study of irradiated $^6\text{Li}$ -formate

K. Komaguchi<sup>a,\*</sup>, Y. Matsubara<sup>a</sup>, M. Shiotani<sup>a</sup>, H. Gustafsson<sup>b</sup>, E. Lund<sup>b</sup>, A. Lund<sup>c</sup>

<sup>a</sup> Graduate School of Engineering, Hiroshima University, Higashi-Hiroshima 739-8527, Japan

<sup>b</sup> Department of Medicine and Care, Radiation Physics, Faculty of Health Sciences, Linköping University, S-581 85 Linköping, Sweden

<sup>c</sup> Chemical Physics Laboratory, IFM, Linköping University, S-581-83 Linköping, Sweden

Received 6 October 2005; accepted 26 April 2006

### Abstract

Lithium formate ( $^6\text{LiOOCH}\cdot\text{H}_2\text{O}$ ), 95%  $^6\text{Li}$  enrichment, combined with an exchange of crystallization water with  $\text{D}_2\text{O}$  was investigated. The ESR spectrum of the radiation induced free radicals stable at room temperature consists of a singlet with a narrow line width, 0.92 mT.  $^6\text{Li}$  has smaller magnetic moment and nuclear spin, which resulted in the narrower line width accompanied with an increase in peak amplitude. In comparison with lithium formate with natural isotopic composition,  $^6\text{Li}$  (7.5%,  $I=1$ ) and  $^7\text{Li}$  (92.5%,  $I=3/2$ ), the sensitivity was increased by a factor of two. With optimised spectrometer settings  $^6\text{Li}$  formate had seven times higher sensitivity compared to alanine. Therefore this material is proposed as a dosimeter material in a dose range down to 0.1 Gy. The  $g$  and the  $^{13}\text{C}$ -hyperfine (hf) tensors of the  $\text{CO}_2^-$  radical anion, major paramagnetic products, were evaluated to be  $g=(2.0037, 1.9975, 2.0017)$ , and  $A(^{13}\text{C})=(465.5, 447.5, 581.3)$  MHz for polycrystalline samples at room temperature. Furthermore, the  $^1\text{H}$ -hf and  $^6\text{Li}$ -hf tensors observed for the surroundings of  $\text{CO}_2^-$  by ENDOR technique were in fairly good agreement with DFT calculations. The  $\text{CO}_2^-$  radicals are found to be so stable that the formate is applicable to the ESR dosimetry, because of fully relaxing in a fully relaxed geometrical structure of the  $\text{CO}_2^-$  component and remaining tight binding with the surroundings after the H atom detachment from  $\text{HCO}_2^-$ .

© 2006 Elsevier B.V. All rights reserved.

**Keywords:**  $^6\text{Li}$ -formate;  $\text{CO}_2^-$  radical anion; ESR; ENDOR

### 1. Introduction

In response to a strong requirement of a convenient and high-sensitive dosimeter in the low dose range below 10 Gy, screening studies on materials alternative to alanine in ESR dosimeters have been extensively carried out [1–4]. In the ESR dosimeter, the absorbed dose is determined by measuring the peak-to-peak signal intensity of the first-derivative spectra of radicals. Therefore, the ESR dosimetry has a great advantage over other methods in permitting simple and rapid determination of the radiation dose, the method being non-destructive and convenient for easy-handling of the samples under test. It is believed that the ESR dosimetry has still great room for enhancement of its sensitivity by modifications of the subjected materials, such as isotope exchange or doping with a small amount of metal ions [5–7].

In the ESR dosimetry, materials which give radicals that are stable with a high yield at room temperature in ambient air are favorable in principle; no decay and no conversion to other radicals should occur after irradiation. Furthermore, it is ideal if there is no hyperfine (hf)- and super hf-structures, and no  $g$ -anisotropy causing broadening of the ESR spectra which also should show a slow saturation behavior; in other words, a single line that is hard to be saturated with a high microwave power.

Actually, alanine is well known as a material for practical use as ESR dosimeter in the dose range 3 Gy–100 kGy, because of the prominent features of high-stability of the radicals formed and its tissue equivalency [8,9]. However, the irradiated alanine gives a spectral line shape with five broad lines spread over more than 10 mT, which essentially reduces the sensitivity so as to become inconveniently low in the dose range below a few Gy. Furthermore, radicals generated in irradiated alanine and its derivatives start to saturate at a relatively low microwave power around 7 mW. Another potential drawback is that several radicals remain stable after irradiation at room temperature. In addition, it is well known that zero-dose signals become disturbing in the low dose range [10,11]. The reported procedures to mea-

\* Corresponding author at: Department of Applied Chemistry, Graduate School of Engineering, Hiroshima University, Higashi-Hiroshima 739-8527, Japan. Tel.: +81 82 4247737; fax: +81 82 4245494.

E-mail address: [okoma@hiroshima-u.ac.jp](mailto:okoma@hiroshima-u.ac.jp) (K. Komaguchi).

sure doses down to 0.05 Gy require long recording times and advanced signal treatment [12]. Even with these precautions, alanine seems to be inadequate for practical use. Therefore, alanine has less potential for extending its applicable dose range below several Gy as high-sensitive ESR dosimeters.

In order to enhance the sensitivity of the ESR dosimeter, several promising materials alternative to alanine have been reported [1–7]. Screening research on the validity of a series of these materials as high-sensitive ESR dosimeters have systematically been carried out, partly by our own work on for example, lithium dithionate ( $\text{Li}_2\text{S}_2\text{O}_6$ ) [3,6,7], ammonium tartrate ( $(\text{NH}_4)_2\text{C}_2\text{H}_4\text{O}_6$ ) [3,13–15], ammonium formate ( $\text{NH}_4\text{OOCH}$ ) [16] and lithium formate ( $\text{LiOOCH}\cdot\text{H}_2\text{O}$ ) [6,7,17,18]. Taking particular note of the sensitivity, for instance, potassium dithionate ( $\text{K}_2\text{S}_2\text{O}_6$ ) was found to show an excellent dose response with an ESR intensity that is 10 times higher than that of alanine, especially in the lower dose range of 0.5–10 Gy relevant for radiation therapy [3]. The material is not tissue-equivalent, however.

Among the materials meeting the requirement of tissue equivalence studied previously [6,7], lithium formate ( $\text{LiOOCH}\cdot\text{H}_2\text{O}$ ) is expected to give a higher dose response by isotope exchange: when  $^7\text{Li}$  ( $I=3/2$ ) and/or  $^1\text{H}$  ( $I=1/2$ ) in  $\text{LiOOCH}\cdot\text{H}_2\text{O}$  are exchanged with  $^6\text{Li}$  ( $I=1$ ) and/or  $^2\text{H}$  ( $I=1$ ) isotopes, respectively, because the magnetic moments ( $\mu$ ) of the latter isotopes are ca. three and four times smaller than those of the former, respectively:  $\mu(^2\text{H})/\mu(^1\text{H})=0.31$  and  $\mu(^6\text{Li})/\mu(^7\text{Li})=0.25$ .

In this paper, we report the potential importance of  $^6\text{Li}$  isotope exchanged lithium formate,  $^6\text{LiOOCH}\cdot\text{H}_2\text{O}$ , as a new material for the high-sensitive ESR dosimeter. The superior fundamental performance, such as absorbed dose response and the stability of the ESR signal intensity, were verified by comparison with those of regular Li-formate monohydrate and alanine. Furthermore, the identification of the main radical formed,  $\text{CO}_2^-$ , and its trapping location are discussed based on the ESR and ENDOR spectroscopic data together with theoretical calculations to elucidate its stability.

## 2. Experimental

$^7\text{LiOOCH}\cdot\text{H}_2\text{O}$  and  $\text{D}_3\text{L}\text{-}\alpha\text{-alanine}$  were purchased from Tokyo Kasei Kogyo and Wako Pure Chemical Industries, respectively. They were used without further purification.  $^6\text{LiOOCH}\cdot\text{H}_2\text{O}$  was synthesized by a neutralization reactions via  $^6\text{Li}_2\text{CO}_3$  obtained from  $^6\text{LiCl}$  from Studsvik Instruments as a starting material (see details in Appendix A). Anhydrous  $\text{LiOOCH}$  was prepared by removal of the crystallization water from the monohydrate by heating the powder at  $120^\circ\text{C}$  for 3 h. Heavy water exchanged Li-formate monohydrate,  $\text{LiOOCH}\cdot\text{D}_2\text{O}$ , was prepared from anhydrous  $\text{LiOOCH}$  by recrystallization from heavy water, followed by storage in a desiccator for a few days to become moderately dry. The structure of the crystals was confirmed by X-ray diffraction analysis (M18XHF, MacScience) [19], and the stoichiometry of the water in the monohydrate was examined by thermogravimetry and differential thermal analysis (SSC5200H, Seiko Instruments).

Following grinding, the powder was pressed into a tablet (diameter: 5 mm, height: 5 mm, weight ca. 0.1 g) with a pres-

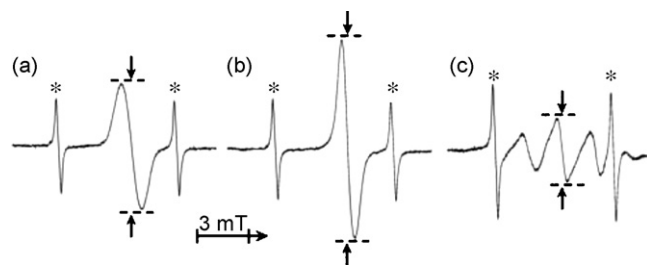


Fig. 1. ESR spectra observed at room temperature for regular  $\text{LiOOCH}\cdot\text{H}_2\text{O}$  (a),  $^6\text{LiOOCH}\cdot\text{H}_2\text{O}$  (b) and alanine (c) irradiated with  $\gamma$ -rays to an absorbed dose of 30 Gy at the same temperature. All the spectra were recorded under the following spectrometer settings, modulation width: 0.32 mT, microwave power: 1 mW, field sweep rate:  $0.083\text{ mT min}^{-1}$ . The spectral intensities were normalized by weight of the samples, and errors caused by the spectrometer instability were corrected by a standard reference of  $\text{Mn}^{2+}/\text{MgO}$  (the hf lines marked as an asterisk) measured together with the sample.

sure of ca.  $100\text{ kg cm}^{-2}$ . The weight of the tablet was accurately measured prior to  $\gamma$ -ray irradiation for the correction of the ESR intensity per weight. The tablets were irradiated with  $\gamma$ -rays from a  $^{60}\text{Co}$  source at room temperature. The quantity of the radiation was converted to the absorbed dose of alanine.

The ESR spectra of the tablets were measured at room temperature on a JEOL JES-RE1X spectrometer together with a standard sample of  $\text{Mn}^{2+}/\text{MgO}$  for correcting spectrometer instability at each measurement (Fig. 1). Unless otherwise noted, all the ESR measurements were performed under fixed spectrometer settings with a modulation width of 0.32 mT at 100 kHz, a microwave power of 1 mW and a magnetic field width of 15 mT with a field sweep rate of  $0.083\text{ mT s}^{-1}$ . The ESR spectra of  $^{13}\text{C}$ -hf structure in natural abundance were measured on a Bruker ESP300E spectrometer. The spectrometer was equipped with a microwave frequency counter 5350B (Hewlett Packard) and an NMR gaussmeter ER035M (Bruker) to calibrate the resonance frequency and magnetic field, respectively. ENDOR spectra were measured at room temperature on a Bruker ESP300E spectrometer with the Bruker ENDOR cavity ( $\text{TM}_{110}$ ) together with a 200 W ENI rf-amplifier (Model 3100LA). The system was set to generate a square-wave-like frequency modulation of the rf-field at 12.5 kHz with a modulation depth of typically 199 kHz.

## 3. Results and discussion

### 3.1. ESR spectra of $\text{LiOOCH}\cdot\text{H}_2\text{O}$

The first-derivative ESR spectra of  $\gamma$ -irradiated regular  $\text{LiOOCH}\cdot\text{H}_2\text{O}$  tablets consist of a singlet with a peak-to-peak linewidth of 1.5 mT at room temperature (Fig. 1(a)). The sensitivity of an ESR dosimeter is essentially determined by the signal-to-noise ratio in the spectra. Therefore, such a singlet line shape is preferable from the viewpoint of realizing a highly sensitive dosimeter, because the intensity is not spread over several hyperfine lines as in the case of irradiated alanine. In fact, the peak-to-peak intensity of the spectra was two times higher than alanine as a reference under identical measurement conditions. The result is in agreement with those reported previously

[3]. Further, the  $G$ -value, the number of radicals formed per 100 eV of energy absorbed on exposure to  $\gamma$ -rays at room temperature, for  $\text{LiOOCH}\cdot\text{H}_2\text{O}$  was evaluated to be ca. 1.2 in the present study. The value is slightly greater than that for alanine, 0.9–0.95 [20,21]. Hence, Li-formate monohydrate is expected to be superior to alanine as the dosimeter in this regard. A detailed investigation of the dosimetric properties of regular  $\text{LiOOCH}\cdot\text{H}_2\text{O}$  using optimized microwave power and modulation parameters was given previously [17].

By the isotopic exchange of  $^7\text{Li}$  ( $I=3/2$ ,  $g_N=2.17$ ) for  $^6\text{Li}$  ( $I=1$ ,  $g_N=0.82$ ), the spectral intensity was further enhanced to four times higher than that of alanine following an accompanying reduction of the linewidth to 0.92 mT (Fig. 1(b)). This is a clear advantage of  $^6\text{Li}$ -formate over alanine, applied to dosimeter materials.

When the crystallization water was substituted for heavy water in regular  $\text{LiOOCH}\cdot\text{H}_2\text{O}$  and  $^6\text{Li}$  enriched  $\text{LiOOCH}\cdot\text{H}_2\text{O}$ , the spectral line shape in the former was little affected by the deuteration, and a minor improvement in resolution and intensity was visible in the latter. It is suggested, therefore, that the magnetic interaction of the unpaired electron with the water protons is not very large. This is in contrast to the result of the  $^6\text{Li}$ -enrichment. On the other hand, the regular  $\text{LiOOCH}$  anhydrate was found to be three times less sensitive than the monohydrate. Consequently, we focused on the monohydrated  $^6\text{LiOOCH}\cdot\text{H}_2\text{O}$  as a dosimeter material in the present study.

### 3.2. Dose dependence

The signal intensity of  $^6\text{LiOOCH}\cdot\text{H}_2\text{O}$  increased linearly with increasing absorbed dose in the dose range from 0.1 to  $1 \times 10^4$  Gy as shown in Fig. 2. The signal intensities of regular  $\text{LiOOCH}\cdot\text{H}_2\text{O}$  and alanine are shown for comparison. To exclude inaccuracy due to its probable progression as discussed below, the ESR intensity was measured within 30 min after com-

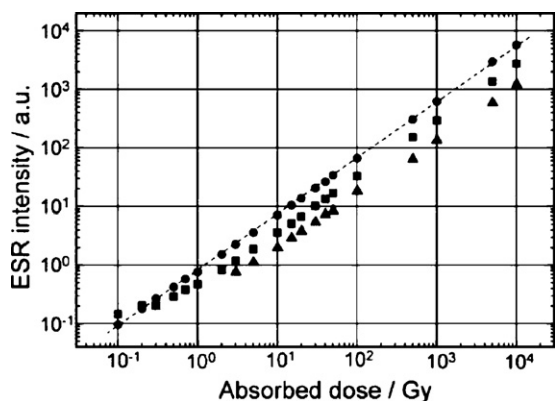


Fig. 2. Dose response of the ESR signal intensity of  $^6\text{Li}$  enriched (●) and regular Li-formate monohydrate (■) irradiated with  $\gamma$ -rays to a dose range of 0.1 Gy–10 kGy at room temperature. For comparison, the plot of alanine (▲) was shown together. The ESR spectra were measured within 30 min after  $\gamma$ -rays irradiation at room temperature. The spectrometer settings were altered on reaching 3 Gy in the dose range; below 3 Gy, modulation width: 1.0 mT, microwave power: 10 mW, above 3 Gy, modulation width: 0.32 mT, microwave power: 1.0 mW. The signal intensity was normalized at a dose of 3 Gy by recording with the two different spectrometer settings.

pletion of irradiation. The spectral settings were altered between the low (<3 Gy) and the high (>3 Gy) dose range; modulation width: 1 and 0.32 mT, microwave power: 10 and 1 mW, below and above 3 Gy, respectively. The signal intensity was normalized at a dose of 3 Gy by recording with the two different spectrometer settings.

In the high dose range between 3 and  $1 \times 10^4$  Gy, the  $y$ -intercepts of the plots at 3 Gy in logarithmic scale coincide with the relative sensitivity to alanine as described above, that is, alanine:  $\text{LiOOCH}\cdot\text{H}_2\text{O}$ :  $^6\text{LiOOCH}\cdot\text{H}_2\text{O} = 1:2:3.9$ . Below 0.3 Gy, the regular  $\text{LiOOCH}\cdot\text{H}_2\text{O}$  deviated from linearity in the double logarithmic plot, putting a lower limit on the detectable dose range for regular  $\text{LiOOCH}\cdot\text{H}_2\text{O}$ . A broad ESR signal extending over several 10 mT, probably due to contaminating paramagnetic metal ion species, in the background signal became prominent in this low dose range. An ESR signal with a wider line width such as that from regular  $\text{LiOOCH}\cdot\text{H}_2\text{O}$  readily interfered with the broad background signal. In contrast with the regular one, the ESR signal of  $^6\text{Li}$ -enriched  $\text{LiOOCH}\cdot\text{H}_2\text{O}$  with a narrower line width resulted in a less serious interference of the background signal in the same dose range. It is clear that the ESR dosimeter of  $^6\text{Li}$ -enriched  $\text{LiOOCH}\cdot\text{H}_2\text{O}$  can precisely detect an irradiated dose as small as 0.1 Gy.

### 3.3. Progression of the signal intensity

The stability of the radicals at room temperature is an important performance requirement for a dosimetry material. The peak-to-peak signal intensity of the irradiated Li-formate was monitored immediately after  $\gamma$ -ray irradiation to a dose of 100 Gy for  $^6\text{LiOOCH}\cdot\text{H}_2\text{O}$  and to a dose of 1 kGy for regular  $\text{LiOOCH}\cdot\text{H}_2\text{O}$  over 2 months at room temperature (Fig. 3).

It is noted here that the stoichiometric excess or deficiency of water in Li-formate monohydrate crystals significantly affect the stability and the yield of radicals, because the water content may readily change substantially depending on the atmospheric humidity. Therefore, careful preparation and treatment of the

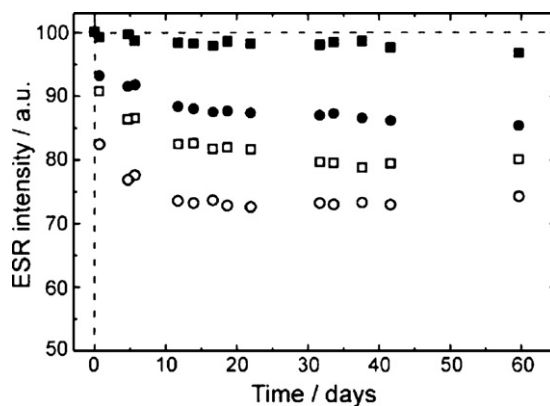


Fig. 3. Time-course of the peak-to-peak ESR signal intensity at room temperature observed for  $\gamma$ -rays irradiated  $\text{LiOOCH}\cdot\text{H}_2\text{O}$  samples. The  $^6\text{LiOOCH}\cdot\text{H}_2\text{O}$  samples were irradiated to a dose of 100 Gy (○) and (●), and the regular  $\text{LiOOCH}\cdot\text{H}_2\text{O}$  samples were irradiated to a dose of 1000 Gy (□) and (■). Two samples were kept in air (○) and (□), and the other samples were each sealed in a glass tube immediately after irradiation (●) and (■).

sample seem to be necessary to keep the stoichiometric water composition in the monohydrate. With this point in view, a couple of identical samples were prepared in order to examine the effect of ambient humidity. One was sealed in air immediately after irradiation to prevent it from further contacting with atmospheric air. Another remained open to the air with a relative humidity of approximately 70% on an average (summer in Hiroshima, 2004). The temperature of the laboratory where the samples were stored and the ESR measurements were done was approximately 26–30 °C.

On exposing the sample to air, open symbols in Fig. 3, the ESR intensity decreased during the first 10 days after irradiation, and from then on the intensity was not very affected. In contrast to this, for the sealed samples, filled symbols, the decrease in intensity was less than for the opened ones. It is obvious that humidity in air can accelerate the decay of the major radicals. The radicals possibly decay out by reacting with excess amount of adsorbed water, which may exist on the surface or in the superficial regions of the crystal. Another point to note is that the decrease in intensity for the regular is smaller than for  $^6\text{Li}$  enriched one. This is because of a high yield of radicals in the regular sample irradiated by 10 times higher dose compared with the  $^6\text{Li}$  enriched sample, not because of a  $^6\text{Li}/^7\text{Li}$  isotope effect. Assuming that the radicals decay out by the reaction with the stoichiometrically excessive water, which is in nearly equal amounts in all samples the fading is expected to become prominent in the low dose irradiated sample. By sealing the irradiated samples, the decrease in signal intensity was effectively suppressed, and more than 96% of the initial intensity remained after 2 months. In a parallel experiment where the Li-formate samples were prepared by degassing and sealing in quartz tubes prior to irradiation, the fading was much less pronounced during the initial several days, despite of relatively low dose irradiation, for instance 3 Gy, comparable to those of Vestad et al. [17].

In conflict with our results, Vestad et al. found that the ESR spectra of  $\text{CO}_2^-$  radical anion present in this material remained unchanged in shape and intensity over a period of 1 week after irradiation, even though the samples are not sealed. This may be because of a lower relative humidity of  $15 \pm 2\%$  in their laboratory [17]. Furthermore, Keizer et al. [22] observed only a weak spectrum due to HCO at room temperature in the irradiated Li-formate in contrast to the strong single line signal detected in this work. The  $\text{CO}_2^-$  radical anion is the major paramagnetic species in the irradiated Li-formate as revealed in the following section. At present, the stability and identification of radicals are not in agreement between the research groups. Therefore, it may need further study of the relationship between characters of the radicals present in the irradiated Li-formate and ambient conditions.

### 3.4. Identification of $\text{CO}_2^-$ radical

When ESR measurements were performed at a microwave power of 4 mW, a modulation amplitude of 0.2 mT and higher amplifier gain to magnify the signal intensity, a couple of satellite signal bands with a separation of ca. 18 mT are clearly observed for the isotopically exchanged Li-formate monohydrate sam-

ples irradiated to a dose of ca. 10 kGy. The ratio of double integrated values of the satellite band to the central singlet was approximately 1:200, which is in accord with the natural isotopic abundance of  $^{13}\text{C}$  ( $I = 1/2$ , 1.1%). Through a line shape analysis of the spectrum in  $^6\text{LiOOCH}\cdot\text{D}_2\text{O}$  which showed the narrowest linewidth among the three different isotopically exchanged samples, the following  $g$ - and  $^{13}\text{C}$ -hf tensors were found to perfectly reproduce the satellite peaks:  $g = (2.0037, 1.9975, 2.0017)$  and  $A = (465.5, 447.5, 581.3)$  MHz (Fig. 4). Further, the central ESR singlet due to  $^{12}\text{C}$  ( $I = 0$ , 98.9%) was fully reproduced using the same  $g$ -tensors as well. The ESR parameters are close to those reported for  $^{13}\text{CO}_2^-$  radical anions generated in irradiated sodium formate ( $\text{NaOOCH}$ ) crystals [23]. The  $^{13}\text{C}$ -hf splitting constants for  $\text{LiOOCH}\cdot\text{H}_2\text{O}$  were larger than that for  $\text{NaOOCH}$  by a factor of ca. 1.07, whereas there were little differences in  $g$ -tensor (2.0032, 1.9975, 2.0014). Recently, one of the authors (A.L.) reported ESR spectra of  $^{13}\text{CO}_2^-$ , but in irradiated regular Li-formate monohydrate [18]. In the present study, the quality of the spectra was much improved by  $^6\text{Li}$  enrichment. The enhanced resolution brought about precise and reliable  $g$ - and  $^{13}\text{C}$ -hf tensors. Through analysis of the tensors, the geometry of the  $\text{CO}_2^-$  radicals and their trapping sites were further elucidated.

The bond angle in the  $\text{CO}_2^-$  radical can be estimated based on the observed  $^{13}\text{C}$ -hf splitting constants because they give the spin

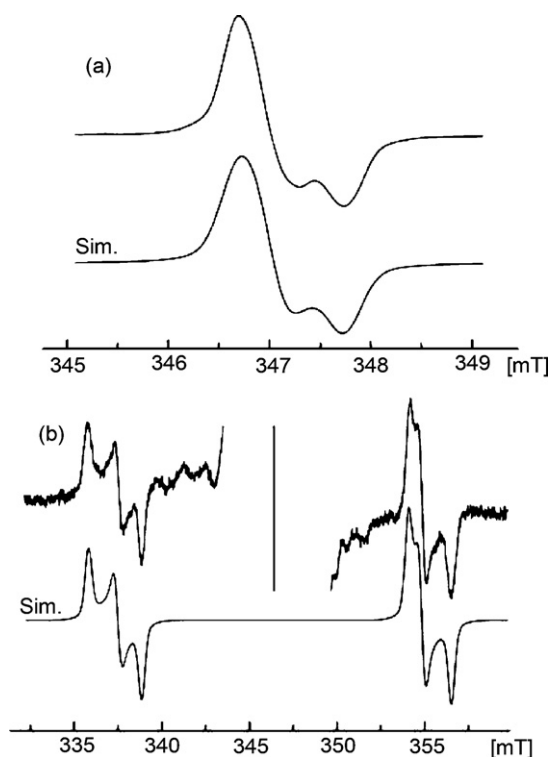
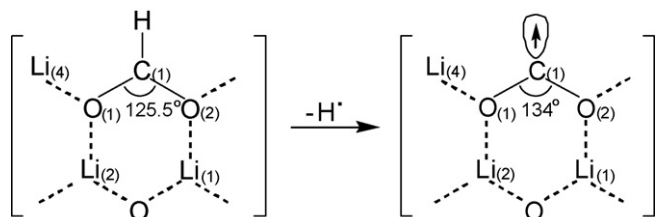


Fig. 4. ESR spectra observed at room temperature for  $^6\text{LiOOCH}\cdot\text{D}_2\text{O}$  irradiated with  $\gamma$ -rays to a dose of 10 kGy. (a) The central part of the spectrum, (b) The spectrum magnified in the vertical direction. The lower spectrum in (a) is the simulated line shape with  $g_1 = 2.0037$ ,  $g_2 = 1.9975$ ,  $g_3 = 2.0017$ ,  $\Delta H_{pp} = 0.37$  mT and taking second order shifts into account.  $^{13}\text{C}$ -hf splitting constants of  $A_1 = 465.5$  MHz,  $A_2 = 447.5$  MHz,  $A_3 = 581.3$  MHz were used for simulating (b) in addition to the same  $g$  and  $\Delta H_{pp}$  values as (a).

density in the 2s- and 2p-orbitals contributing to the hybridization of these orbitals. According to the molecular orbital theory, the singly occupied molecular orbital (SOMO) of  $\text{CO}_2^-$ ,  $\phi(4a_1)$ , is expressed as follows [24,25],

$$\phi(4a_1) = c_1\text{C}(s) + c_2\text{C}(p_z) + c_3\text{O}(p_{z1} + p_{z2}) + c_4\text{O}(p_{y1} - p_{y2}) + c_5\text{O}(s_1 + s_2).$$

Based on Coulson's treatment to analyse the hybridization [26], the angle  $\theta(\text{O}-\text{C}-\text{O})$  is derived from the relation  $\cos \theta = -\lambda^2/(\lambda^2 + 2)$ , where  $\lambda^2$  is the ratio of the hybridization,  $\lambda^2 = c_2^2/c_1^2$ . The atomic orbital coefficients,  $c_1$  and  $c_2$  were experimentally determined as the ratio of the observed isotropic and anisotropic  $^{13}\text{C}$ -hf splitting constants to those for the  $^{13}\text{C}$  2s- and 2p-orbitals with unit spin density, respectively [24]. Consequently, the bond angle,  $\theta$ , was evaluated to be  $134^\circ$ , which is  $8.5^\circ$  larger than the original one,  $125.5^\circ$ , in the crystal [19], as a result of formation of  $\text{CO}_2^-$ . This is in accordance with the reduction in s-p hybridization at the C-atom by the loss of the hydrogen atom. This is also supported by ab initio MO calculations (UHF/6-31G\*\* level of theory) for isolated  $\text{CO}_2\text{H}^-$  and  $\text{CO}_2^-$  systems where the bond angle increased from  $131^\circ$  to  $135^\circ$  by the hydrogen atom detachment. The agreement in the bond angle between the experimental and the theoretical values suggests that the  $\text{CO}_2^-$  component trapped in the crystal is a fully relaxed structure.



### 3.5. ENDOR spectra

The local structure of  $\text{CO}_2^-$  with its surroundings was examined by the ENDOR technique to elucidate stability and formation mechanisms of the radicals. Fig. 5 shows ENDOR spectra observed at room temperature for three isotopically different  $\text{LiOOCH}$  monohydrates,  $\text{LiOOCH}\cdot\text{H}_2\text{O}$ ,  $\text{LiOOCH}\cdot\text{D}_2\text{O}$  and  $^6\text{LiOOCH}\cdot\text{H}_2\text{O}$ . The regular Li samples (Fig. 5(a) and (b)) gave at least four pairs of peaks due to  $^7\text{Li}$  ( $I = 3/2$ ) nuclei, in the external magnetic field locked at the center of the singlet ESR line. The isotropic and anisotropic components in the Li-hf structure were evaluated by ENDOR line shape simulation methods [27]. The calculated line shapes that best fitted the experimental ones are shown in the figure. The corresponding hf splitting constants due to  $^6\text{Li}$  ( $I = 1$ ) nuclei, reduced by a factor of  $1/2.64$ , were observed for the  $^6\text{Li}$  enriched sample (Fig. 5(c)), and the line shape was successfully reproduced using the scaled hf parameters. The Li-hf splitting constants observed in the present study are summarized in Table 1. For comparison, the previous values from a single crystal ENDOR study are also shown in the table. The present isotropic and anisotropic values obtained at room temperature show a tendency to be by one to several %

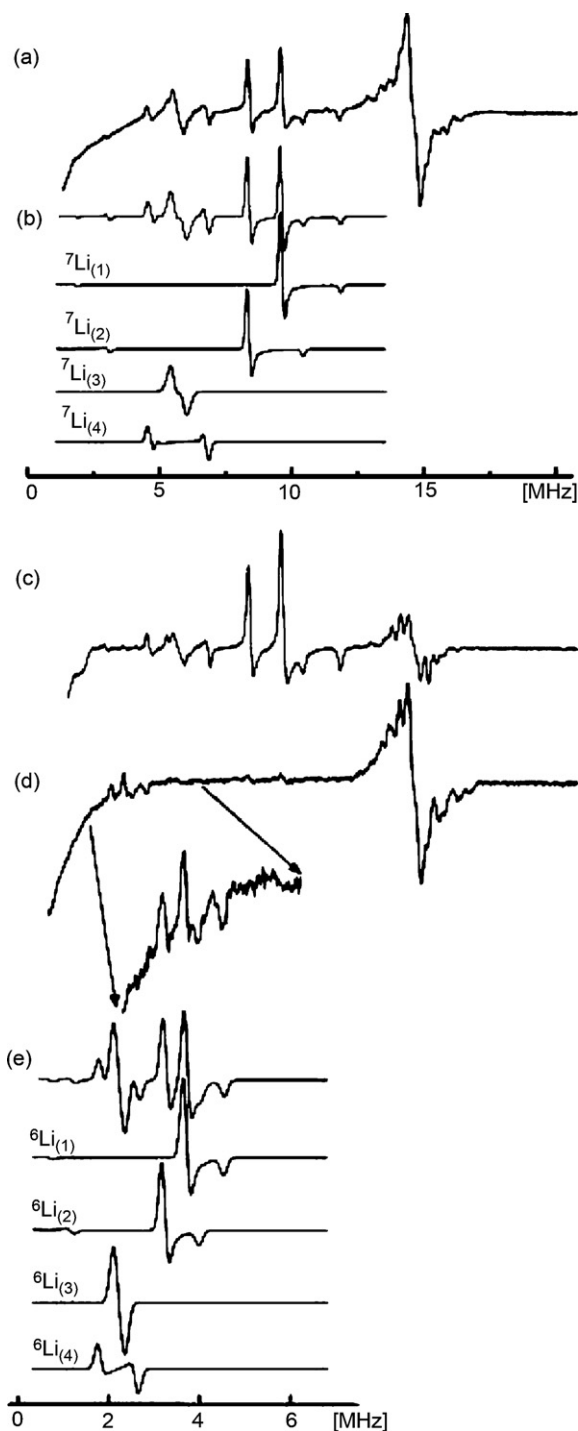


Fig. 5. ENDOR spectra observed at room temperature for  $\text{LiOOCH}\cdot\text{H}_2\text{O}$  (a),  $\text{LiOOCH}\cdot\text{D}_2\text{O}$  (c),  $^6\text{LiOOCH}\cdot\text{H}_2\text{O}$  (d) irradiated with  $\gamma$ -rays to a dose of 10 kGy. The composite line shapes, (b) and (e), were calculated for (a) and (d), respectively, which are obtained by adding four simulated line shapes due to magnetically different Li-nuclei,  $\text{Li}_{(1)}$ ,  $\text{Li}_{(2)}$ ,  $\text{Li}_{(3)}$  and  $\text{Li}_{(4)}$ .

larger in magnitude than those at low temperature, indicating a temperature effect on the magnitudes of the coupling constants.

In addition, multiple lines comprised of at least four different pairs of peaks appeared centering around the ENDOR frequency of the free proton (Fig. 5). The resolution of the proton ENDOR was improved by  $^6\text{Li}$  enrichment and the deuteration of crystal-

Table 1

$^7\text{Li}$ -hf splitting constants (in MHz) of an irradiated  $\text{LiOOCH}\cdot\text{H}_2\text{O}$  polycrystalline sample observed by ENDOR technique at room temperature, together with theoretical values calculated for the surrounding  $^7\text{Li}$  ions in the vicinity of the  $\text{CO}_2^-$  radical (in parentheses)

$a_{\text{iso}}$	$b_1$	$b_2$	$b_3$
$\text{Li}_{(1)}$			
9.80 (8.09)	1.588 <sup>a</sup> (1.739)	1.588 <sup>a</sup> (1.366)	3.176 (3.105)
9.70	1.495		2.99
$\text{Li}_{(2)}$			
7.07 (6.24)	1.467 <sup>a</sup> (1.593)	1.467 <sup>a</sup> (1.332)	2.934 (2.925)
6.85	1.39		2.78
$\text{Li}_{(3)}$			
0.0 (0.174)	0.533 (0.0021)	0.420 (0.0021)	0.953 (0.0042)
0.01	0.445		0.89
$\text{Li}_{(4)}$			
-0.972 (-1.006)	1.523 (1.524)	1.159 (1.207)	2.683 (2.731)
-0.92	2.19		2.53

The theoretical calculations were done for a model structure consisting of 113 atoms at B3LYP/3-21G\* level of theory, where the central  $\text{CO}_2^-$  radical was optimized at the same level of theory and other atoms were fixed in the same positions as in the undamaged  $\text{LiOOCH}\cdot\text{H}_2\text{O}$  crystal. For comparison, the hf values reported by Vestad et al. [18] are shown in the second line of each entry.

<sup>a</sup> The observed hf values are assumed to be axially symmetric.

lization water, but the peaks due to non-exchangeable protons and the separation between them are likely independent of the deuteration. The result is consistent with the ESR observations that the interaction between  $\text{CO}_2^-$  and crystallization water was negligibly small. Even though the resolution is slightly higher than in regular  $\text{LiOOCH}\cdot\text{H}_2\text{O}$ , the assignment of the  $^1\text{H}$ -hf splitting becomes ambiguous at this point, because of the difficulty in identifying the corresponding couples of anisotropic peaks. The second radical suggested by Vestad et al. [18] as a less abundant species was not detected in the present study.

### 3.6. Possible location of $\text{CO}_2^-$

Based on the axially symmetric hf-tensor of Li-nuclei observed by ENDOR, the local structure of  $\text{CO}_2^-$  trapped in the  $\text{LiOOCH}\cdot\text{H}_2\text{O}$  crystal was further examined. A probable trapping site for  $\text{CO}_2^-$  has previously been proposed by comparison of the orientations of the  $^7\text{Li}$ -hf principal directions derived from single crystal ENDOR data with the positions in the undamaged crystal [18]. In the present work, isotropic and anisotropic hf values were theoretically evaluated by the DFT method for Li nuclei in the proximity of the  $\text{CO}_2^-$  radical. The model crystalline structure used in the calculations consists of the central  $\text{CO}_2^-$  anion and its surroundings (113 atoms in total) as shown in Fig. 6. The coordinates of all the surrounding atoms were fixed at positions identical with those of the undamaged crystalline lattice, which structure has been reported in a neutron diffraction study [19]. Then, a hydrogen atom was removed from the central  $\text{HCO}_2^-$  component to form the  $\text{CO}_2^-$  radical anion, for which the coordinates of the molecule were subjected to a full geometrical optimization at B3LYP/3-21G\* level of theory using the Gaussian 03 program [28]. For the optimized structure, the bond lengths,  $\text{C}_{(1)}-\text{O}_{(1)}$  and  $\text{C}_{(1)}-\text{O}_{(2)}$ , were evaluated

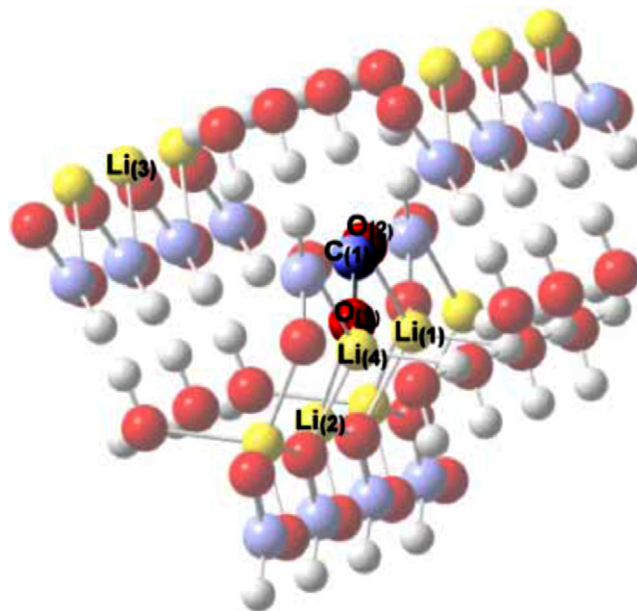


Fig. 6. Schematic representation of trapping site of  $\text{CO}_2^-$  radical anion generated in an orthorhombic  $\text{LiOOCH}\cdot\text{H}_2\text{O}$  crystal. The whole structure composed of 113 atoms was used as a model for the calculations, where the high-lighted  $\text{CO}_2^-$  fragment,  $\text{O}_{(1)}-\text{C}_{(1)}-\text{O}_{(2)}$ , was geometrically optimized and the surroundings were kept at the same positions as in the undamaged crystal. The atoms are numbered according to the previous work [18].

to be 127.5 and 126.3 pm. Both bonds are elongated compared to those of the  $\text{HCO}_2^-$  group, but the elongation is quite small. On the other hand, in accordance with the above conclusion based on the experimental  $^{13}\text{C}$ -hf splitting constants, the bond angle,  $\text{O}_{(1)}-\text{C}_{(1)}-\text{O}_{(2)}$  was evaluated to be  $129.56^\circ$ , which is larger by  $4^\circ$  than that in the undamaged crystalline structure. Further, it was revealed by the calculations that no appreciable shift in the mass center of the  $\text{CO}_2^-$  component could be accompanied by the H atom detachment; the shift was at most 2.5 pm from the original position. The theoretical results suggest, consequently that the  $\text{CO}_2^-$  radical is fixed as tightly as the original location of undamaged  $\text{HCO}_2^-$  and its bond angle increases only by several degrees. This may be one of the primary reasons why the formed  $\text{CO}_2^-$  radical is stable enough to make the system applicable as a high-sensitive dosimeter.

The  $^7\text{Li}$ -hf values were calculated at the same level of theory for the model structure where the  $\text{CO}_2^-$  geometry was optimized in the fixed surrounding framework. Comparing the magnitude and sign of the calculated isotropic hf values with the experimental ones, the observed four different Li-nuclei were assigned as summarized in Table 1. There is a fairly good agreement between the calculated and observed values; the experimental isotropic hf splitting constants of 9.80, 6.85, 0.0 and  $-0.97$  MHz were attributable to  $\text{Li}_{(1)}$ ,  $\text{Li}_{(2)}$ ,  $\text{Li}_{(3)}$  and  $\text{Li}_{(4)}$  ions, whose locations are shown in Fig. 6, with the corresponding theoretical values, 8.09, 6.24, 0.174,  $-1.006$  MHz, respectively. The good agreement further supports the calculated  $\text{CO}_2^-$  geometrical structure with quite small shifts from the original one of  $\text{HCO}_2^-$ . Furthermore, the assignment supports the validity of the previous results on Li-hf assignment using a point dipole approximation by Vestad et al. [18].

#### 4. Conclusions

The ESR and ENDOR study revealed that  $^6\text{Li}$  enriched lithium formate monohydrate,  $^6\text{LiOOCH}\cdot\text{H}_2\text{O}$ , is a promising material applicable to high-sensitive ESR dosimetry. The decrease in line width by a factor of 0.61 (0.92 mT) compared with that of ordinary  $\text{LiOOCH}\cdot\text{H}_2\text{O}$  (1.5 mT) was attained by the  $^6\text{Li}$  enrichment: the signal intensity was seven to eight times stronger than the alanine under the optimized spectrometer settings for each sample, and the intensity linearly increased with the absorbed dose in the low dose range from around 0.1 Gy. On the other hand, the deuteration of crystallization water little affected the signal intensity. By the accompanying enhancement of the ESR intensity and resolution, we evaluated accurate ESR parameters of the  $\text{CO}_2^-$  radical anion, formed in irradiated  $^6\text{LiOOCH}\cdot\text{D}_2\text{O}$ , as a major paramagnetic species. Further, ENDOR observations revealed that at least four different Li nuclei are located in the vicinity of the  $\text{CO}_2^-$  radical in agreement with the previous study by Vestad et al. [18]. Based on the observed  $^6\text{Li}$ - and  $^{13}\text{C}$ -hf splitting constants compared with theoretical DFT calculations, the  $\text{CO}_2^-$  radicals are located at almost the same position as the  $-\text{OOCH}$  component in the undamaged crystal, except that the  $\text{O}-\text{C}-\text{O}$  bond angle was estimated, experimentally, to increase to  $134^\circ$  due to the H atom detachment, which is close to that predicted by DFT for an isolated  $\text{CO}_2^-$  molecule. It was apparent that the  $\text{CO}_2^-$  anions are highly stabilized as a relaxed form through tight binding with the surrounding  $\text{Li}^+$  ions, and less with protons of crystallization water, in accord with the ESR observations.

#### Acknowledgements

We thank Professor S. Yamanaka and Dr. H. Fukuoka for their help of the Li-formate crystalline powder XRD measurements and analysis. A  $^6\text{LiCl}$  sample was donated by Studsvik Instruments. This work was supported in part by the grant from STINT (the Swedish Foundation for International Cooperation in Research and Higher Education) and Wenner-Gren foundation.

#### Appendix A

$^6\text{Li}_2\text{CO}_3$  was synthesized as the starting material for the synthesis of  $^6\text{LiOOCH}\cdot\text{H}_2\text{O}$  through the reaction of  $^6\text{LiCl}$  (2.1 g) with excess amount of  $\text{Na}_2\text{CO}_3$  (~12 g) in water.  $^6\text{Li}_2\text{CO}_3$  is less soluble in water on increasing temperature, contrary to  $\text{NaCl}$  as the by-product, which is more soluble with temperature, so that the mixture solution was warmed up to near  $100^\circ\text{C}$  to separate  $^6\text{Li}_2\text{CO}_3$  crystals from the solution by filtration. After giving twice rinses with hot water, the  $^6\text{Li}_2\text{CO}_3$  crystals were mixed with an excess amount of  $\text{HCOOH}$  in distilled water, and then anhydrous  $^6\text{LiOOCH}$  crystals were obtained by evaporation of the water together with  $\text{HCOOH}$  and  $\text{CO}_2$  as by-products at  $160^\circ\text{C}$ . Finally, the  $^6\text{LiOOCH}\cdot\text{H}_2\text{O}$  crystals were recrystallized from water by keeping it in a desiccator at room temperature.

#### References

- [1] M. Ikeya, T. Miki (Eds.), *ESR Dating and Dosimetry*, Ionics Pub, Tokyo, 1985.
- [2] M. Ikeya, in: M.R. Zimmerman, N. Whitehead (Eds.), *New Applications of Electron Spin Resonance: Dating, Dosimetry and Microscopy*, World Scientific, Singapore, 1993.
- [3] A. Lund, S. Olsson, M. Bonora, E. Lund, H. Gustafsson, *Spectrochim. Acta A* 58 (2002) 1301.
- [4] N.D. Jordanov, V. Gancheva, in: A. Lund, M. Shiotani (Eds.), *EPR of Free Radicals in Solids*, Kluwer Academic Pub., Dordrecht, 2003, pp. 565–599.
- [5] M. Ikeya, G.M. Hassan, H. Sasaoka, Y. Kinoshita, S. Takaki, C. Yamanaka, *Appl. Radiat. Isot.* 52 (2000) 1209.
- [6] E. Lund, H. Gustafsson, M. Danilczuk, M.D. Sastry, A. Lund, T.A. Vestad, E. Malinen, E.O. Hole, E. Sagstuen, *Appl. Radiat. Isot.* 62 (2005) 317.
- [7] E. Lund, H. Gustafsson, M. Danilczuk, M.D. Sastry, A. Lund, *Spectrochim. Acta A* 60 (2004) 1319.
- [8] W.W. Bradshaw, D.G. Cadena, G.W. Crawford, H.A. Spetzler, *Radiat. Res.* 17 (1962) 11.
- [9] D.F. Regulla, U. Deffner, *Int. J. Appl. Radiat. Isot.* 33 (1982) 1101.
- [10] E. Sagstuen, E.O. Hole, S.R. Haugedal, W.H. Nelson, *J. Phys. Chem. A* 101 (1997) 9763.
- [11] E. Malinen, M.Z. Heydari, E. Sagstuen, E.O. Hole, *Radiat. Res.* 159 (2003) 23.
- [12] F. Ruckerbauer, M. Sprunck, D.F. Regulla, *Appl. Radiat. Isot.* 47 (1996) 1263.
- [13] S.K. Olsson, S. Bagherian, E. Lund, G.A. Carlsson, A. Lund, *Appl. Radiat. Isot.* 50 (1999) 955.
- [14] M. Brustolon, A. Zoleo, A. Lund, *J. Mag. Res.* 137 (1999) 389.
- [15] S.K. Olsson, E. Lund, A. Lund, *Appl. Radiat. Isot.* 52 (2000) 1235.
- [16] H. Gustafsson, S. Olsson, A. Lund, E. Lund, *Radiat. Res.* 161 (2004) 464.
- [17] T.A. Vestad, E. Malinen, A. Lund, E.O. Hole, E. Sagstuen, *Appl. Radiat. Isot.* 59 (2003) 181.
- [18] T.A. Vestad, H. Gustafsson, A. Lund, E.O. Hole, E. Sagstuen, *Phys. Chem. Chem. Phys.* 6 (2004) 3017.
- [19] R. Tellgren, P.S. Ramanujam, R. Liminga, *Ferroelectrics* 6 (1974) 191.
- [20] G.M. Hassan, M. Ikeya, S. Toyoda, *Appl. Radiat. Isot.* 49 (1998) 823.
- [21] M.A. Sharaf, G.M. Hassan, *Nucl. Instr. Meth. in Phys. Rev. B* 217 (2004) 603.
- [22] P.N. Keizer, J.R. Morton, K.F. Preston, *J. Chem. Soc. Faraday Trans.* 87 (1991) 3147.
- [23] G.W. Chantray, A. Horsfield, J.R. Morton, D.H. Whiffen, *Mol. Phys.* 5 (1962) 233.
- [24] D.W. Overall, D.H. Whiffen, *Mol. Phys.* 4 (1961) 135.
- [25] K. Sogabe, A. Hasegawa, Y. Yamada, M. Miura, *Bull. Chem. Soc. Jpn.* 45 (1972) 3362.
- [26] C.A. Coulson, *Contribution a l'etude de la Structure Moleculaire*, Victor Henri Volume Commemoratif, 1948, p. 15.
- [27] A. Lund, R. Erickson, *Acta Chem. Scand.* 52 (1998) 261.
- [28] M.J. Frisch, G.W. Trucks, H.B. Schlegel, G.E. Scuseria, M.A. Robb, J.R. Cheeseman, J.A. Montgomery Jr., T. Vreven, K.N. Kudin, J.C. Burant, J.M. Millam, S.S. Iyengar, J. Tomasi, V. Barone, B. Mennucci, M. Cossi, G. Scalmani, N. Rega, G.A. Petersson, H. Nakatsuji, M. Hada, M. Ehara, K. Toyota, R. Fukuda, J. Hasegawa, M. Ishida, T. Nakajima, Y. Honda, O. Kitao, H. Nakai, M. Klene, X. Li, J.E. Knox, H.P. Hratchian, J.B. Cross, V. Bakken, C. Adamo, J. Jaramillo, R. Gomperts, R.E. Stratmann, O. Yazyev, A.J. Austin, R. Cammi, C. Pomelli, J.W. Ochterski, P.Y. Ayala, K. Morokuma, G.A. Voth, P. Salvador, J.J. Dannenberg, V.G. Zakrzewski, S. Dapprich, A.D. Daniels, M.C. Strain, O. Farkas, D.K. Malick, A.D. Rabuck, K. Raghavachari, J.B. Foresman, J.V. Ortiz, Q. Cui, A.G. Baboul, S. Clifford, J. Cioslowski, B.B. Stefanov, G. Liu, A. Liashenko, P. Piskorz, I. Komaromi, R.L. Martin, D.J. Fox, T. Keith, M.A. Al-Laham, C.Y. Peng, A. Nanayakkara, M. Challacombe, P.M.W. Gill, B. Johnson, W. Chen, M.W. Wong, C. Gonzalez, J.A. Pople, *Gaussian 03, Revision B. 05*, Gaussian, Inc., Wallingford CT, 2004.